

## Research Article

## Study on the Effect of Fabrication Method on the Polarization of Solid Oxide Fuel Cells

A. Karimi and M.H. Paydar\*

Department of Materials Science and Engineering, School of Engineering, Shiraz University, Shiraz, Iran

## ARTICLE INFO

*Article history:*

Received 2 January 2025  
 Reviewed 8 February 2025  
 Revised 9 February 2025  
 Accepted 18 February 2025

*Keywords:*

Electrochemical impedance spectroscopy  
 Freeze casting  
 Polarization resistance  
 SOFC

*Please cite this article as:*

Karimi, A., & Paydar, M. H. (2025). Study on the effect of fabrication method on the polarization of solid oxide fuel cells. *Iranian Journal of Materials Forming*, 12(1), 4-9. <https://doi.org/10.22099/IJMF.2025.52070.1316>

## ABSTRACT

A promising strategy for reducing concentration polarization in solid oxide fuel cells (SOFCs) is the creation of an anode layer with aligned, channel-like pores to facilitate efficient gas transport with minimal resistance. Freeze casting is an advanced shaping technique capable of forming such a unique microstructure. In this study, three NiO-YSZ|YSZ|LSM-YSZ SOFCs were fabricated using three different methods, and their electrochemical performances were compared. The first cell featured an anode prepared via freeze casting, while the other two utilized conventional dry pressing; one with a pore former and other one without. All anodes were composed of NiO-50 wt.% YSZ composite powder, with YSZ electrolyte and LSM-YSZ cathode layers subsequently applied. The microstructures were analyzed using scanning electron microscopy (SEM), and electrochemical impedance spectroscopy was conducted within the 650–800 °C temperature range. The concentration polarization resistance of the freeze-cast anode-supported SOFC was 0.09 and 0.07  $\Omega\cdot\text{cm}^2$  at 750 and 800 °C, respectively. At 800 °C, concentration polarization resistance was accounted for 13% of total cell resistance in the freeze-cast anode SOFC, compared to 20% and 22% in the dry-pressed anodes with and without a pore former, respectively.

© Shiraz University, Shiraz, Iran, 2025

### 1. Introduction

Solid oxide fuel cells (SOFCs) are a promising green energy technology, but their commercialization depends on achieving sufficient reliability. These fuel cells operate at high temperatures (700-1000 °C), enabling efficient fuel-to-electricity conversion with energy efficiencies exceeding 60%. Additionally, SOFCs can use a variety of fuels, including hydrogen, natural gas,

and biofuels, making them suitable for diverse applications. Their low emissions and ability to operate on carbon-neutral fuels further enhance their benefits [1-3].

A major challenge in SOFC operation is polarization, which leads to voltage losses and efficiency reductions due to electrochemical and transport processes. There are three main types of polarization in SOFCs: ohmic,

\* Corresponding author  
 E-mail address: [paaydar@shirazu.ac.ir](mailto:paaydar@shirazu.ac.ir) (M.H. Paydar)  
<https://doi.org/10.22099/IJMF.2025.52070.1316>

activation, and concentration polarization. Ohmic polarization arises from ionic resistance in the electrolyte and electrodes. Activation polarization is caused by sluggish electrochemical reactions at the electrode surface. Concentration polarization occurs when reactant depletion near the electrode surface limits cell performance [4-6].

Among these, concentration polarization is particularly problematic and has significantly hindered SOFC commercialization. This issue occurs at the electrode-electrolyte interface, reducing efficiency and overall performance. To address this, researchers have explored various strategies, including microstructural optimization of SOFC components and the use of freeze casting to enhance reactant transport and minimize polarization losses [7, 8].

The microstructure of key SOFC components, such as the electrode and electrolyte, plays a significant role in overall performance. By tailoring the microstructure, mass transport properties can be enhanced, reducing concentration polarization. Freeze casting is a promising technique that enables the controlled solidification of a dispersed phase to create highly porous materials with aligned structures. This method provides precise control over the three-dimensional architecture, porosity, and pore connectivity, making it an effective strategy for improving SOFC efficiency and performance.

Freeze casting has been successfully used to develop SOFCs with low mass transfer resistance and excellent electrochemical performance [9, 10]. This technique enables the fabrication of functionally graded acicular support structures that facilitate gas diffusion through channels formed by ice crystal growth [11, 12]. At NASA Glenn Research Center, freeze-cast planar single cells are expected to achieve an exceptionally high specific power density of  $1.0 \text{ kW kg}^{-1}$ , attributed to the low tortuosity of acicular pores in the anode support [13]. Gannon et al. [14] developed planar freeze-cast NiO-8YSZ anodes with functionally graded porosity, columnar structures, and embedded nanoparticles. Additionally, freeze tape-casting has been used to create Ni-8YSZ anodes with controlled porosity, achieving a power output of  $1.28 \text{ W.cm}^{-2}$  and a polarization

resistance of just  $0.166 \text{ }\Omega\text{.cm}^2$  at  $800 \text{ }^\circ\text{C}$  using hydrogen as fuel and ambient air as the oxidant. This setup utilized Ni-YSZ as the anode, YSZ as the electrolyte, and LSM-YSZ as the cathode [15]. Chen et al. [10] further optimized SOFC performance by developing a highly efficient cell incorporating a freeze-cast Ni-GDC anode, a gadolinia-doped ceria (GDC) electrolyte, and an infiltrated freeze-cast GDC backbone cathode. The Ni-GDC anode was fabricated using freeze tape-casting, while the hierarchically porous cathode, featuring  $\text{SrSc}_{0.1}\text{Co}_{0.9}\text{O}_{3-\delta}$  (SSC) nanoparticles on a needle-like GDC framework, was created through a combination of freeze tape-casting and self-rising methods. The resulting cells demonstrated an impressive peak power density of  $1.44 \text{ W.cm}^{-2}$  and a low polarization resistance of  $0.0379$  at  $600 \text{ }^\circ\text{C}$ .

This paper provides a comprehensive overview of fabrication techniques and strategies for reducing concentration polarization by engineering the SOFCs anode microstructure through freeze casting. It explores various microstructural modifications, including freeze casting and dry pressing methods, and their impact on cell polarization resistance. Furthermore, the study examines the impact of freeze casting on SOFC components microstructure and its role in mitigating concentration polarization.

## 2. Experimental Procedure

### 2.1. Fabrication of planar anode substrates by freeze casting and dry press methods

Nickel oxide (NiO) (Merck), yttria-stabilized zirconia (8YSZ), and lanthanum strontium manganite (LSM) (Inframent Advanced Materials Co) were used in this study.

Anode samples were fabricated using the freeze casting method with a slurry containing 15 vol.% of NiO-50 wt.% 8YSZ powder mixture. The freezing rate was set at  $3 \text{ }^\circ\text{C/min}$ , following previously reported methods [16]. For comparison, two additional anode samples were prepared using the dry pressing method, with and without a pore former (graphite), as summarized in Table 1. All anode samples had a 20 mm diameter and were pre-sintered at  $1200 \text{ }^\circ\text{C}$  for 2 hours.

**Table 1.** Details of the three different cells used in this study

Cells	Anode	Anode fabrication method	Electrolyte (spin coating)	Cathode (Brush painting)
Cell I	NiO-YSZ	Freeze-casting	YSZ	LSM-YSZ
Cell II	NiO-YSZ-20 wt.% graphite as pore former	Dry-press	YSZ	LSM-YSZ
Cell III	NiO-YSZ	Dry-press	YSZ	LSM-YSZ

### 2.2. Fabrication of anode-supported SOFC

The YSZ electrolyte layer was applied to the anode substrate using the spin coating method with a 5 wt.% YSZ slurry. The anode–electrolyte assembly was then co-sintered at 1400 °C for 5 hours [17]. The LSM-8YSZ cathode layer was deposited onto the electrolyte using a brush-painting method and subsequently baked at 1100 °C for 2 hours. To facilitate electrical conductivity, silver paste was applied to both sides of the cell as a current-collecting layer, covering a surface area of 0.196 mm<sup>2</sup>.

### 2.3. Characterization and electrochemical measurements

The microstructure of the fabricated cells was analyzed using a scanning electron microscope (SEM, VEGA TESCAN). The size and distribution of pores in the NiO-8YSZ anode supporting layer of the cells were determined using SEM imaging.

Electrochemical impedance measurements were conducted using a Solartron 1287 electrochemical interface coupled with a Solartron 1260 frequency response analyzer. The SOFCs were tested with hydrogen as the fuel and oxygen as an oxidant, supplied at flow rate of 30 ml/min and 50 ml/min, respectively. The complex impedance of the cells was measured over

a frequency range of 1 mHz to 1 MHz.

## 3. Results and Discussion

### 3.1. Structural properties of Ni-YSZ anodes

The scanning electron microscope (SEM) image of the freeze-cast anode supporting solid oxide fuel cell (SOFC) for Cell I (Fig. 1) reveals a microstructure characterized by columnar or lamellar arrangements formed by ice crystals. As shown in Fig. 1, the freeze-cast lamella walls exhibit a distribution of pore size and lamella thickness, with interlamellar pore sizes ranging from 10 to 20 μm. SEM analysis of Cell II shows pores oriented perpendicular to the pressing axis, formed due to the removal of graphite from the structure after baking. These pores, ranging from 10 to 20 μm in length, are uniformly distributed throughout the structure. In contrast, Cell III exhibits distinct individual pores within the anode layer. Notably, all three cells demonstrate satisfactory adhesion and continuity between the anode/electrolyte and electrolyte/cathode layers. Additionally, the electrolyte layer in all samples displays uniform thickness and proper sintering.

### 3.2. Electrochemical performance of anode-supported SOFCs

Fig. 2 illustrates the electrochemical impedance spectroscopy (EIS) diagram of cells fabricated using different methods, measured over the temperature range of 650-800 °C. The intersection of the graph with the horizontal axis in the low frequency region represents the ohmic resistance of the cell.

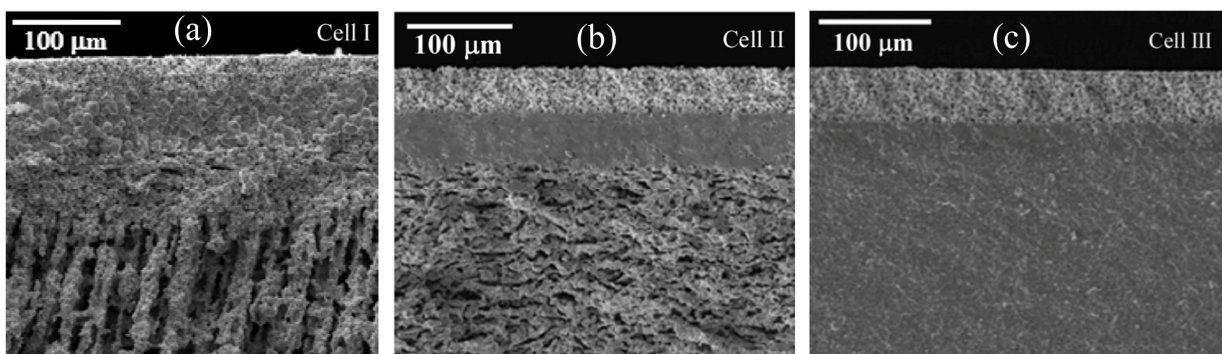


**Fig. 1.** SEM images of Cell I, Cell II, and Cell III.

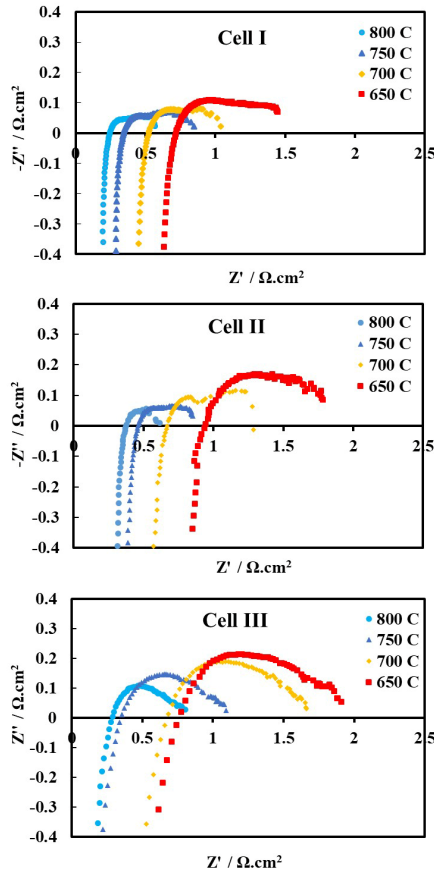


Fig. 2. Electrochemical impedance spectroscopy (EIS) diagrams of Cell I, II, and III measured in the temperature range of 650-800 °C.

Additionally, the high-frequency intercept with the real axis corresponds to the total cell resistance, while the difference between these two values determines the interfacial polarization resistance ( $R_p$ ) [18, 19]. As illustrated in Fig. 2, Cell I exhibits a lower polarization resistance than Cell II and Cell III, indicating improved electrochemical performance.

### 3.3. Concentration polarization resistance of anode-supported SOFCs

An equivalent circuit, as shown in Fig. 3, was used to separate the polarization resistances. This circuit comprises of three resistors, a capacitor, two constant phase elements (CPE), and an inductor. The values of these elements were determined using Z-view software.  $R_o$  represents the ohmic resistance of the cells, which increases as temperature decreases, primarily impacting the electrolyte's ohmic resistance [20]. In Fig. 4, the resistance of Cell I is plotted against temperature.

$R_1$  and  $R_2$  vary with temperature, whereas  $R_3$  remains relatively constant despite temperature fluctuations. Thus,  $R_1$  and  $R_2$  correspond to activation polarization resistance, while  $R_3$  represents concentration polarization resistance. At 800 °C, the concentration polarization resistance ( $R_3$ ) values for Cell I, Cell II, and Cell III are 0.07, 0.12, and 0.18  $\Omega.cm^2$ , respectively. As shown in Table 2, the results indicate that Cell I shows a lower polarization resistance compared to the cells manufactured using the dry pressing method.

Fig. 5 shows the ratio of concentration polarization resistance to total cell resistance ( $R_3/R_t$ ) for Cell I, Cell II, and Cell III. For Cell I, the values at 650, 700, 750, and 800 °C are 0.13, 0.11, 0.08, and 0.07  $\Omega.cm^2$ , respectively. Table 2 also displays this ratio for Cell II and Cell III, demonstrating higher values than Cell I. This trend suggests that as temperature decreases, activation polarization becomes more dominant, leading to a reduction in the  $R_3/R_t$  ratio.

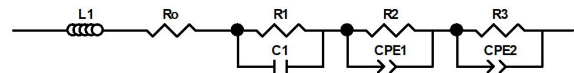


Fig. 3. Equivalent circuit model used to determine the polarization resistances of cells.

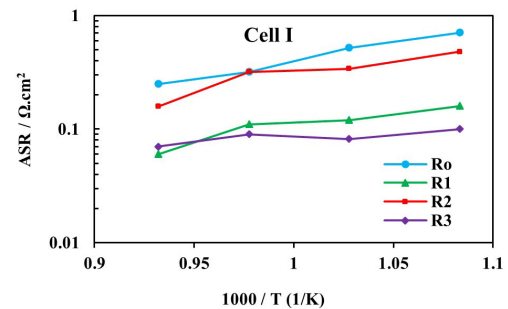


Fig. 4. Variation of resistance components (area-specific resistance (ASR)) in Cell I as a function of temperature.

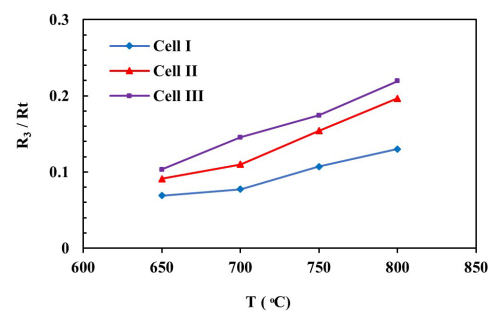


Fig. 5. Contribution of concentration polarization resistance to total cell resistance.

Table 2. Polarization resistance values for Cell I, Cell II, and Cell III

	T (° C)	R <sub>o</sub> (Ω.cm <sup>2</sup> )	R <sub>1</sub> (Ω.cm <sup>2</sup> )	R <sub>2</sub> (Ω.cm <sup>2</sup> )	R <sub>3</sub> (Ω.cm <sup>2</sup> )	R <sub>p</sub> (Ω.cm <sup>2</sup> )	R <sub>t</sub> (Ω.cm <sup>2</sup> )	R <sub>3</sub> /R <sub>t</sub>
<b>Cell I</b> Freeze- cast anode	800	0.25	0.06	0.158	0.07	0.288	0.538	0.13
	750	0.32	0.11	0.32	0.09	0.52	0.84	0.11
	700	0.521	0.12	0.34	0.082	0.542	1.063	0.08
	650	0.707	0.16	0.48	0.1	0.74	1.447	0.07
<b>Cell II</b> Dry press anode with graphite	800	0.39	0.06	0.04	0.12	0.22	0.61	0.20
	750	0.46	0.134	0.12	0.13	0.384	0.844	0.15
	700	0.67	0.17	0.31	0.142	0.622	1.292	0.11
	650	0.93	0.31	0.22	0.146	0.676	1.606	0.09
<b>Cell III</b> Dry press anode	800	0.29	0.1	0.25	0.18	0.53	0.82	0.22
	750	0.35	0.24	0.31	0.19	0.74	1.09	0.17
	700	0.58	0.34	0.43	0.23	1	1.58	0.15
	650	0.75	0.27	0.63	0.19	1.09	1.84	0.10

#### 4. Conclusions

The microstructure of anode-supported SOFCs was successfully evaluated using freeze casting and dry pressing methods for the anode layer. The electrolyte and cathode layers were effectively applied using spin coating and brush painting methods, respectively.

Electrochemical impedance spectroscopy (EIS) analysis was conducted to determine the polarization resistance using an equivalent circuit model. The results indicated that concentration polarization resistance remained relatively stable across different temperatures, whereas ohmic and activation polarization varied with temperature. Among the three tested cells, Cell I—fabricated using the freeze casting method—exhibited the lowest concentration polarization resistance. This suggests that freeze-cast anode structure enhances fuel gas diffusion, leading to improved SOFC performance.

#### Acknowledgments

The authors gratefully acknowledge Shiraz University for providing financial support during the research work.

#### Conflict of interest

The authors declare no conflict of interest.

#### Funding

This research was funded by the Shiraz University.

#### 5. References

- [1] Singh, M., Zappa, D., & Comini, E. (2021). Solid oxide fuel cell: Decade of progress, future perspectives and challenges. *International Journal of Hydrogen Energy*, 46(54), 27643-27674. <https://doi.org/10.1016/j.ijhydene.2021.06.020>
- [2] Owusu, P. A., & Asumadu-Sarkodie, S. (2016). A review of renewable energy sources, sustainability issues and climate change mitigation. *Cogent Engineering*, 3(1), 1167990. <https://doi.org/10.1080/23311916.2016.1167990>
- [3] Gadsbøll, R. Ø., Thomsen, J., Bang-Møller, C., Ahrenfeldt, J., & Henriksen, U. B. (2017). Solid oxide fuel cells powered by biomass gasification for high efficiency power generation. *Energy*, 131, 198-206. <https://doi.org/10.1016/j.energy.2017.05.044>
- [4] Zhao, F., & Virkar, A. V. (2005). Dependence of polarization in anode-supported solid oxide fuel cells on various cell parameters. *Journal of Power Sources*, 141(1), 79-95. <https://doi.org/10.1016/j.jpowsour.2004.08.057>
- [5] Tsepis, E. V., & Kharton, V. V. (2011). Electrode materials and reaction mechanisms in solid oxide fuel cells: a brief review. III. Recent trends and selected methodological aspects. *Journal of Solid State Electrochemistry*, 15, 1007-1040. <https://doi.org/10.1007/s10008-011-1341-8>
- [6] Fleig, J. (2003). Solid oxide fuel cell cathodes: Polarization mechanisms and modeling of the electrochemical performance. *Annual Review of Materials Research*, 33(1), 361-382. <https://doi.org/10.1146/annurev.matsci.33.022802.093258>

- [7] Bae, Y., Lee, S., & Hong, J. (2019). The effect of anode microstructure and fuel utilization on current relaxation and concentration polarization of solid oxide fuel cell under electrical load change. *Energy conversion and management*, 201, 112152. <https://doi.org/10.1016/j.enconman.2019.112152>
- [8] Jeon, D. H., Nam, J. H., and Kim, C. J. (2006). Microstructural optimization of anode-supported solid oxide fuel cells by a comprehensive microscale model. *Journal of the Electrochemical Society*, 153(2), A406. <https://doi.org/10.1149/1.2139954>
- [9] Bunch, J., Chen, Y., Chen, F., & May, M. (2012). Freeze-tape casting for the design of anode-delivery layer in solid oxide fuel cells. In P. Singh & N. P. Bansal (Ed.), *Advances in solid oxide fuel cells VIII* (pp. 13-21). John Wiley & Sons.
- [10] Chen, Y., Liu, Q., Yang, Z., Chen, F., & Han, M. (2012). High performance low temperature solid oxide fuel cells with novel electrode architecture, *RSC Advances*, 2(32), 12118-12121. <https://doi.org/10.1039/C2RA21921B>
- [11] Souza, D. F., Nunes, E. H., & Vasconcelos, W. L. (2018). Preparation of  $\text{Ba}_{0.5}\text{Sr}_{0.5}\text{Co}_{0.8}\text{Fe}_{0.2}\text{O}_{3-\delta}$  asymmetric structures by freeze-casting and dip-coating. *Ceramics International*, 44(1), 1002–1006. <https://doi.org/10.1016/j.ceramint.2017.10.035>
- [12] Sofie, S. W. (2007). Fabrication of functionally graded and aligned porosity in thin ceramic substrates with the novel freeze-tape-casting process. *Journal of the American Ceramic Society*, 90(7), 2024–2031. <https://doi.org/10.1111/j.1551-2916.2007.01720.x>
- [13] Cable, T. L., Sofie, S. W. (2007). A symmetrical, planar SOFC design for NASA's high specific power density requirements. *Journal of Power Sources*, 174(1), 221–227. <https://doi.org/10.1016/j.jpowsour.2007.08.110>
- [14] Gannon, P., Sofie, S., Deibert, M., Smith, R., & Gorokhovskiy, V. (2008). Thin film YSZ coatings on functionally graded freeze cast NiO/YSZ SOFC anode supports, *Journal of Applied Electrochemistry*, 39, 497–502. <https://doi.org/10.1007/s10800-008-9682-4>
- [15] Chen, Y., Bunch, J., Li, T., Mao, Z., & Chen, F. (2012). Novel functionally graded acicular electrode for solid oxide cells fabricated by the freeze-tape-casting process, *Journal of Power Sources*, 213, 93–99. <https://doi.org/10.1016/j.jpowsour.2012.03.109>
- [16] Karimi, A., & Paydar, M. H. (2024). Investigation on the mechanical behavior and fracture mode of ice-templated NiO-ysz anode electrode for solid oxide fuel cells application. *Journal of Materials Engineering and Performance*, 33(13), 6499–6506. <https://doi.org/10.1007/s11665-023-08419-x>
- [17] Talebi, T., Haji, M., & Raissi, B. (2010). Effect of sintering temperature on the microstructure, roughness and electrochemical impedance of electrophoretically deposited YSZ electrolyte for SOFCs. *International Journal of Hydrogen Energy*, 35(17), 9420-9426. <https://doi.org/10.1016/j.ijhydene.2010.05.079>
- [18] Nakajima, H., Kitahara, T., & Konomi, T. (2010). Electrochemical impedance spectroscopy analysis of an anode-supported microtubular solid oxide fuel cell. *Journal of the Electrochemical Society*, 157(11), B1686. <https://doi.org/10.1149/1.3486805>
- [19] Wang, B., Bi, L., & Zhao, X. (2018). Fabrication of one-step co-fired proton-conducting solid oxide fuel cells with the assistance of microwave sintering. *Journal of the European Ceramic Society*, 38(16), 5620-5624. <https://doi.org/10.1016/j.jeurceramsoc.2018.08.020>
- [20] Liu, M., Dong, D., Peng, R., Gao, J., Diwu, J., Liu, X., & Meng, G. (2008). YSZ-based SOFC with modified electrode/electrolyte interfaces for operating at temperature lower than 650 C. *Journal of Power Sources*, 180(1), 215-220. <https://doi.org/10.1016/j.jpowsour.2008.01.066>